

MICROSTRUCTURAL EXAMINATION OF IRRADIATED VANADIUM ALLOYS - D. S. Gelles (Pacific Northwest National Laboratory)^a and H. M. Chung (Argonne National Laboratory)

OBJECTIVE

The objective of this effort is to provide collaborative understanding of microstructural evolution in irradiated vanadium alloys for first wall applications in a fusion power system.

SUMMARY

Microstructural examination results are reported for a V-5Cr-5Ti unirradiated control specimen of heat BL-63 following annealing at 1050°C, and V-4Cr-4Ti heat BL-47 irradiated in three conditions from the DHCE experiment: at 425°C to 31 dpa and 0.39 appm He/dpa, at 600°C to 18 dpa and 0.54 appm He/dpa and at 600°C to 18 dpa and 4.17 appm He/dpa.

PROGRESS AND STATUS

Introduction

Vanadium is being developed for application as a first wall material for fusion power system. It has been shown that an alloy of composition V-4Cr-4Ti has optimum properties¹ and the effort has shifted to demonstration that properties provide an adequate design window. However, degradation of properties has been observed in some heats of V-5Cr-5Ti as a result of high temperature annealing,^{2,3} and results from the Dynamic Helium Charging Experiment (DHCE) to determine consequences of helium production during irradiation require further investigation to understand microstructural evolution.^{4,5} The present effort was initiated in order to develop interlaboratory collaboration and to investigate two issues: the cause of degraded properties in one heat of V-4Cr-4Ti (Heat BL-63), and the microstructure of a heat of V-4Cr-4Ti (BL-47) following irradiation in the DHCE experiment. The microstructural evolution in the latter heat included both precipitation response as a function of temperature and effects of a different rate of helium production on bubble development.

Experimental Procedure

Four specimens were selected for examination: a control specimen of heat BL-63 following annealing at 1050°C for 1 h in high vacuum, and three irradiated specimens of heat BL-47 from the DHCE experiment: at 425°C to 31 dpa and 0.39 appm He/dpa, at 600°C to 18 dpa and 4.17 appm He/dpa, and at 600°C to 18 dpa and 0.54 appm He/dpa. Heat compositions are provided in Table 1 and irradiation conditions in Table 2. Specimens selected for examination had been examined previously^{2,4,5} and had been stored for over a year in a standard laboratory desiccator without any apparent degradation. Examinations were performed on a JEOL 100CX at ANL.

Results

The control specimen of V-5Cr-5Ti heat BL-63 following annealing at 1050°C was examined to determine if unusual microstructures were developing at grain boundaries following heat treatment. A typical grain boundary was examined in a number of dark field imaging conditions, with both grains

^aOperated for the U.S. Department of Energy by Battelle Memorial Institute under Contract DE-AC06-76RLO 1830.

Table 1. Composition of Heats Examined

Heat #	Nominal Composition	Concentration [ppm]			
		O	N	C	Si
BL-63	V-4.6Cr-5.1Ti	440	28	73	310
BL-47	V-4.1Cr-4.3Ti	350	220	200	870

Table 2. Irradiation conditions for DHCE specimens of V-4Cr-4Ti (BL-47) examined.

Packet Code	Irradiation Temperature (°C)	Fluence (n/cm ²)	Dose (dpa)	Helium (appm)	Helium production (appm He/dpa)
4D1	425	6.4x10 ²²	31	11.2-13.3	0.39
5C1	600	3.7x10 ²²	18	8.4-11.0	0.54
5C2	600	3.7x10 ²²	18	74.9-75.3	4.17

diffracting. In each case, the grain boundary region was strongly visible in dark field using non-matrix reflections. The most extreme case, where the strong dark field image was obtained for a very small \vec{g} , is shown in Figure 1. Figure 1 provides comparison of a boundary in bright field (a) and in dark field (b) (at a different position of tilt) with the diffraction condition inset showing the aperture position by a double exposure procedure. It was eventually concluded that this imaging condition was a result of double diffraction and therefore misleading. The bright field image shows distortions in the grain boundary thickness fringes probably characteristic of the grain boundary precipitation observed in previous studies.^{2,3}

The specimen of V-4Cr-4Ti heat BL-47 irradiated in the DHCE experiment at 425°C to 31 dpa and 0.39 appm He/dpa was examined to provide further understanding of the microstructure and precipitation formed during irradiation. Attempts to produce precipitate dark field images were unsuccessful due to the small size of the precipitate and the resultant weak diffraction spots. Effort was therefore shifted to record microstructural features. A low magnification image of bubbles or voids associated with grain boundaries near a node is provided in Figure 2 (a). Boundaries are not straight, indicating that migration took place during irradiation. The bubbles appear as equiaxed white circular features, most often near but not on the boundary. Figures 2 (b) and (c) provide comparison of another region in $\vec{g} = \langle 011 \rangle$ strain contrast near (011) and in void contrast, respectively, adjacent to a grain boundary. Strain contrast reveals curved dislocation line segments, typical of climbing dislocations, small equiaxed features as large as 5 nm that are probably precipitates, and circular features with dark rings most common near the boundary that can be shown by comparison with Figure 2 (c) to probably be bubbles. Again, bubbles are non-uniformly distributed. Stereoscopic examination showed that several bubbles were on the boundary, but many were not. Figure 2 (c) also reveals precipitation on the order of 4 nm in diameter. The precipitate is only imaged at surfaces and appears typical of a phase formed by solute segregation. It is anticipated that this phase is rich in titanium, silicon and phosphorus.^{6,7}

The specimens of V-4Cr-4Ti heat BL-47 irradiated in the DHCE experiment at 600°C to 18 dpa and 0.54 appm He/dpa and at 600°C to 18 dpa and 4.17 appm He/dpa were examined to provide further understanding of the effect of helium generation on microstructural development and to further

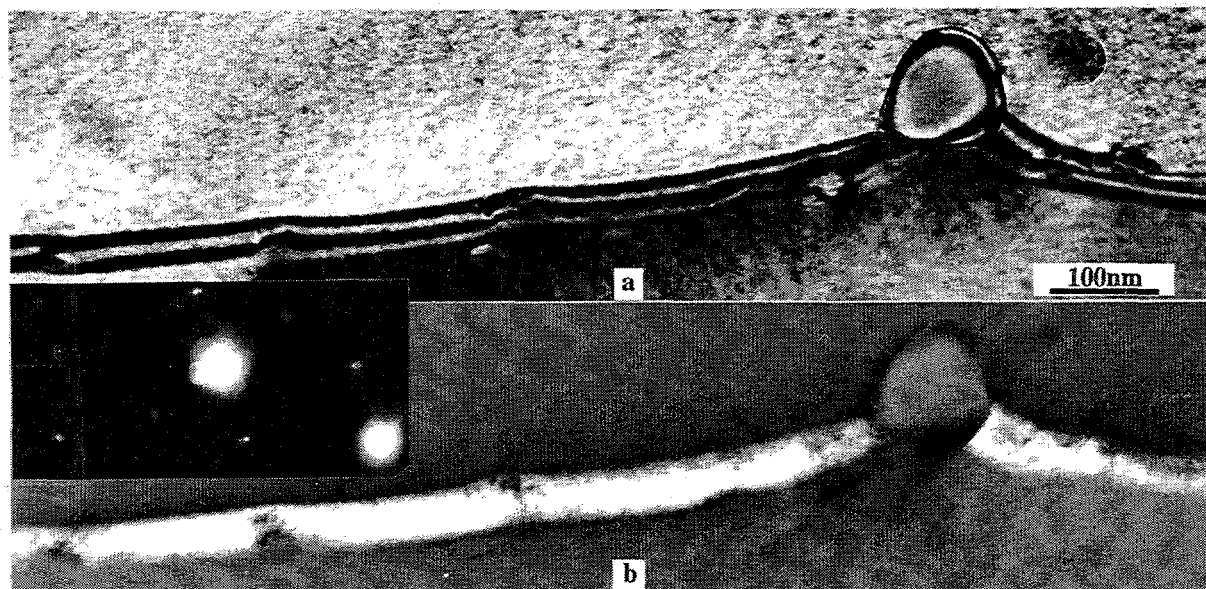


Figure 1. Imaging of grain boundary structure in a specimen of V-5Cr-5Ti heat BL-63 following annealing at 1050°C in bright field (a) and dark field (b).

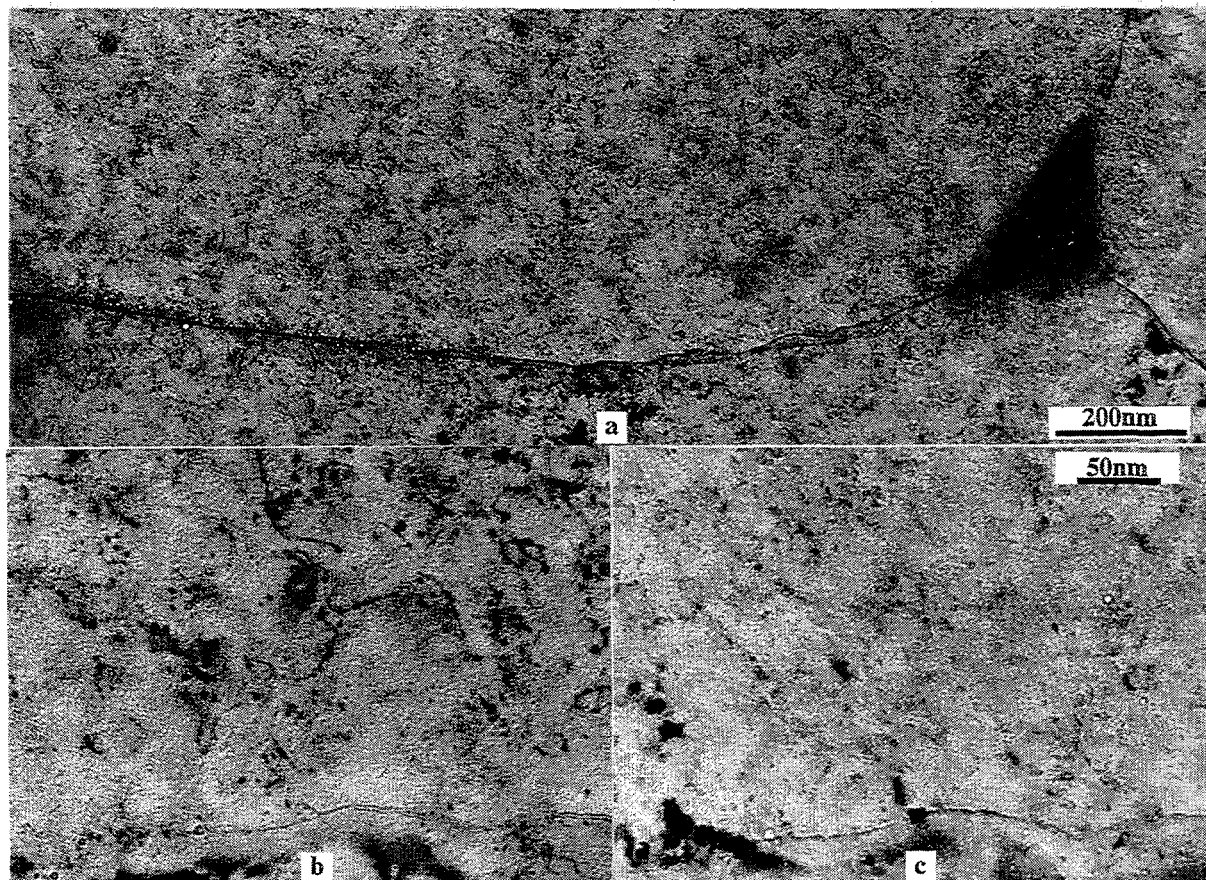


Figure 2. Microstructure of a specimen of V-5Cr-5Ti heat BL-47 following irradiation in the DHCE experiment at 425°C to 31 dpa and 0.39 appm He/dpa showing bubbles near grain boundaries at low magnification in (a) and structure near a grain boundary at higher magnification in dislocation contrast (b) and void contrast (c).

elucidate precipitation response. It was found that both conditions contained bubbles or voids, but densities and sizes were low. A low magnification example for the condition containing about 75 appm He is given in Figure 3 (a), and only a low density of small bubbles on the order of 7 nm can be identified in the matrix. However, careful comparison of boundary features in the two conditions, shown in Figures 3 (b) and (c) indicate a different distribution of helium bubbles. A few bubbles as large as 7 nm can be identified in the upper center of Figure 3 (b) for the specimen containing 10 appm He whereas a much higher density of smaller 3.5 nm bubble-like features can be observed in Figure 3 (c) for the specimen containing 75 appm He. Therefore, higher helium levels appear to promote local regions of higher densities of smaller bubbles, with maximum bubble sizes about the same in both cases.

Microstructural evolution at 600°C differed from that at 425°C primarily with regard to precipitate development. Dislocation structure consisted of loops and curved dislocation line segments, typical of climbing dislocations. Precipitates were elongated and as large as 40 nm long and 7 nm wide, and were easily imaged using, for example, $\frac{3}{4} \langle 200 \rangle$. However, differences could not be identified as function of helium production. Examples of the microstructures are provided in Figures 3 (d) and (e) for the specimen from packet 5C1 containing 10 appm He and in Figures 3 (f) and (g) for the specimen from packet 5C2 containing 75 appm He. In both cases, $\bar{g} = \langle 200 \rangle$ contrast was used for the bright field image and $\bar{g} = \frac{3}{4} \langle 200 \rangle$ for the precipitate dark field image. The corresponding diffraction pattern is inset into Figure 3 (e) showing the typical elongation of the diffraction spot. Note that the operating \bar{g} is perpendicular to the sense of elongation, indicating that the shape is probably plate-like, seen on edge. It is anticipated that this phase is TiP⁶ based on the $\frac{3}{4} [200]$ reflection, but similar morphologies have been identified previously as Ti₅Si₃.⁴ Therefore, further investigation is necessary to identify the precipitate.

Discussion

The microstructural examinations reported here, although incomplete, agree with previously reported results on these or similar specimens.^{4,6} However, the precipitate development found as a function of irradiation temperature and heat-to-heat variations in minor impurities should be taken into account because precipitation involves different chemical species at different temperatures. Such a response can arise because a precipitate becomes unstable above a critical temperature, but disappearance of a phase at lower temperatures is unusual unless precipitate dissolution is occurring due to cascade mixing, a phenomenon not generally found unless the irradiation temperatures are very low, and often leading to amorphization.

This work provides the novel observation that from the DHCE experiment it is found that increased helium levels may lead to a higher density of smaller helium bubbles in localized regions that can be overlooked because of their size. Mechanical property testing appears to show however that such increases in bubble density have little effect on deformation response.⁸

CONCLUSIONS

Collaborative microstructural examinations have been performed on a V-5Cr-5Ti control specimen of heat BL-63 following annealing at 1050°C, and specimens of V-4Cr-4Ti heat BL-47 irradiated in three conditions from the DHCE experiment: at 425°C to 31 dpa and 0.39 appm He/dpa, at 600°C to 18 dpa and 0.54 appm He/dpa and at 600°C to 18 dpa and 4.17 appm He/dpa. Results demonstrate that images of grain boundaries in BL-63 showing continuous coatings of unexpected phases are probably a result of double diffraction. Double diffraction effects must be ruled out before such images can be accepted as arising from precipitation. In BL-47 irradiated in DHCE, increases in helium generation may have

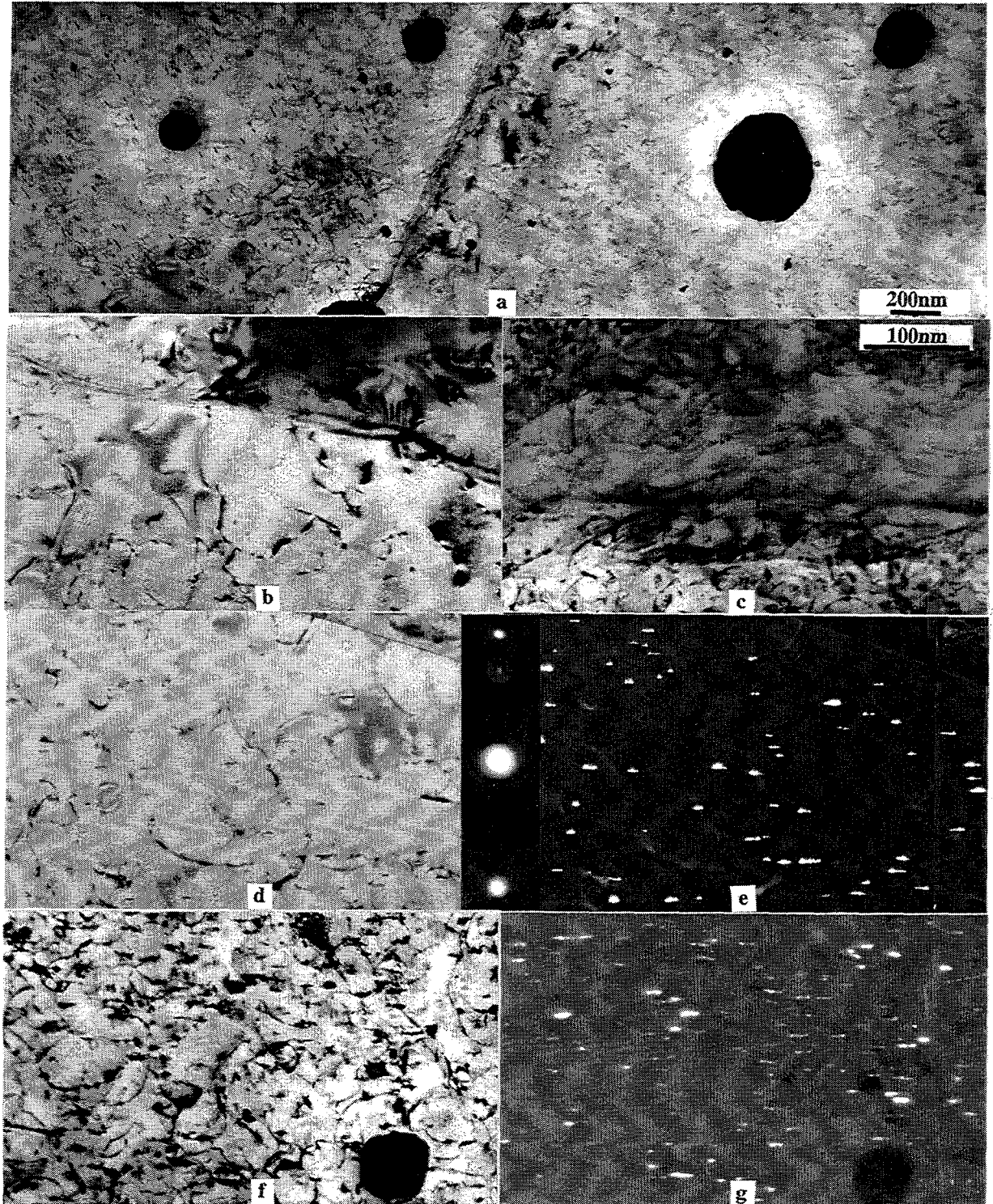


Figure 3. Microstructures of a specimens of V-5Cr-5Ti heat BL-47 following irradiation in the DHCE experiment at 600°C to 18 dpa and 0.54 or 4.17 appm He/dpa showing bubbles near grain boundaries at low magnification with 75 appm He in (a), bubbles near a grain boundary at higher magnification with 10 appm He in (b) and 75 appm He in (c), dislocation and precipitate structures with 10 appm He in (d) and (e) and with 75 appm He in (f) and (g).

resulted in high densities of smaller bubbles. However, precipitation response as a function of temperature is not completely understood.

Future work

It is planned to shift this collaborative work to the JEOL 2010F at PNNL in order to provide microchemical analysis when specimens and funding are available.

Acknowledgements

The authors acknowledge the help of Larry Nowicki for specimen transfers and support.

REFERENCES

1. B. A. Loomis, A. B. Hull, and D. L. Smith, J. Nucl. Mater., 179-181 (1992) 148.
2. H. M. Chung, J. Gazda, L. J. Nowicki, J. E. Sanecki, and D. L. Smith, DOE/ER-0313/15, 207
3. D. S. Gelles and Huaxin Li, DOE/ER-0313/19, 22
4. H. M. Chung, B. A. Loomis, H. Tsai, L. J. Nowicki, J. Gazda, and D. L. Smith, DOE/ER-0313/16, 204
5. H. M. Chung, L. J. Nowicki, J. Gazda, and D. L. Smith, DOE/ER-0313/17, 211.
6. H. M. Chung and D. L. Smith, J. Nucl. Mater., 191-194 (1992) 942.
7. H. M. Chung, B. A. Loomis, and D. L. Smith, J. Nucl. Mater., 212-215 (1994) 804.
8. H. M. Chung, B. A. Loomis, L. J. Nowicki, and D. L. Smith, DOE/ER-0313/19, 77.